

# Hybrid Propulsion In-Situ Resource Utilization Test Facility Results

Ashley Chandler Karp<sup>1</sup> Barry Nakazono<sup>2</sup>, David Vaughan<sup>3</sup> and William N. Warner<sup>4</sup>  
Jet Propulsion Laboratory, California Institute of Technology

Hybrid rockets present a promising alternative to conventional chemical propulsion systems for In-Situ Resource Utilization (ISRU) and in-space applications. While they have many benefits for these applications, there are still many small details that require research before they can be adopted into flight systems. A flexible test facility was developed at JPL to test operation of hybrid motors at small scale (5 cm outer diameter fuel grains) over a range of conditions. Specifically, this paper studies two of the major advantages: low temperature performance and throttling. Paraffin-based hybrid rockets are predicted to have good performance at low temperatures. This could significantly decrease the overall system mass by minimizing the thermal conditioning required for Mars or outer planet applications. Therefore, the coefficient of thermal expansion and glass transition of paraffin are discussed. Additionally, deep throttling has been considered for several applications. This was a natural starting point for hotfire testing using the hybrid propulsion ISRU test facility. Additionally, short length to diameter ratio ( $L/D$ ) fuel grains are tested to determine if these systems can be packaged into geometrically constrained spaces.

## Nomenclature

$\alpha$	=	coefficient of thermal expansion (CTE)
$f$	=	frequency
$G_o$	=	oxidizer mass flux
$L$	=	length of fuel port
$O/F$	=	oxidizer to fuel ratio
$P_c$	=	chamber pressure
$RT_{avg}$	=	average gas constant temperature product

## I. Introduction

HYBRID rocket propulsion is a promising candidate for a variety of in-space applications. Research in this field has been revitalized recently thanks to the strong advantages associated with these systems (e.g. high performance, storability, throttleability, and restartability) coupled with the high regression rate fuels discovered in the late 1990's. However, in general, they remain at fairly low technology readiness level (TRL) and commercial off the shelf (COTS) in-space hybrid motors do not exist. Most designs for in-space hybrid motors remain relatively immature, with several parameters open for interpretation.

A Mars Simulating Hybrid *In-Situ* Propulsion test facility has been designed and built at NASA's Jet Propulsion Laboratory (JPL) and was described in Ref. 1. The facility was designed for flexibility in testing. Many variables can be altered, including: fuel and oxidizer type, mass flow rate, length to diameter ratio of the fuel grain, oxidizer to fuel ratio, etc. Additionally, a spin casting set up capable of making up to 5 cm (2 in) outer diameter fuel grains was developed at JPL this year and the fuel grains for tests 5-8 were cast in house. Prior fuel grains were cast for JPL by Stanford University.

---

<sup>1</sup> Propulsion Engineer, JPL Propulsion and Fluid Flight Systems, M/S 125-211, AIAA Member

<sup>2</sup> Senior Propulsion Engineer, JPL Propulsion and Fluid Flight Systems, M/S 125-211, AIAA Member

<sup>3</sup> Group Supervisor, JPL Propulsion and Fluid Flight Systems, M/S 125-211, AIAA Member

<sup>4</sup> Technologist, JPL Analytical Chemistry and Materials Development, M/S 125-109

Several technologies are investigated here to further the capability of paraffin-based hybrids for future Mars applications. The low temperature performance of hybrid fuels has often been predicted as favorable. Material testing was conducted on paraffin wax to shed some light on the glass transition. The coefficient of thermal expansion over a range of temperatures applicable to Mars surface missions is discussed. Additionally, throttling is believed to be a useful technology. Therefore, low oxidizer mass fluxes are investigated to determine performance during throttling. Four tests are presented here to discuss the behavior of such systems at low oxidizer flow rates. Both supercritical and subcritical chamber pressures are evaluated.

## II. Test Set Up

### A. Hybrid Propulsion In-Situ Resource Utilization Test Facility

The hybrid rocket test facility at JPL is displayed in Figure 1. The tests reported here were run with paraffin wax and gaseous oxygen. However, it is also possible to test alternative fuels or introduce varying concentrations of CO<sub>2</sub> and CO into the oxidizer feed system to determine the performance impact on ISRU contaminants. All tests are conducted at ambient external pressure and temperatures. Temperatures in Southern California are typically between 15 and 30 °C and are recorded for each test along with the humidity level.

Fuel grains made of high melt temperature wax from the Candlewic company (160F Melt Point – 5560 paraffin wax). They are centrifugally cast at JPL using a dedicated casting system. All fuel grains were made of the paraffin and a black dye. The fuel grains are made with a roughly 2:1 outer to inner diameter ratio. However, stresses in the wax are clearly visible. Some small surface cracks appear along the port of the fuel grain. Other researchers have solved this problem with strength additives, which may be a subject for future work. However, for the present tests, the fuel grains were burned with the surface cracks and it was noted that a relatively smooth layer is left after each test. The fuel grains are about 5.1 cm (2 in) diameter by 15.2 cm (6 in) long, which results in a 3:1 length to diameter ratio. The combustion chamber is 20.3 cm (8 in) long, which accommodates the fuel grain, plus a 5.1 cm (2 in) post combustion chamber. This can be varied in future tests.

The feed system introduces oxidizer and purge gas (N<sub>2</sub>) into the system. A sonic orifice just upstream of the injector sets the oxidizer flow rate. The four tests presented in Section IV use the same orifice (4.34 mm<sup>2</sup> area) and injector (4.60 mm<sup>2</sup> area). These areas are fairly close in size. Future tests will have a larger separation between the two cross sectional areas to ensure that the flow is choking at the orifice and not the injector and that the oxidizer enters the combustion chamber subsonically.



**Figure 1. Hybrid Test Facility Set Up.** *Current configuration utilizes GOx and N<sub>2</sub> as a purge.*

The oxidizer mass flow rate is calculated from the upstream temperature and pressure coupled with the differential pressure across a custom venturi. The oxidizer mass flow calculations were validated by running cold flows and measuring the delta mass of the oxygen cylinder. The mass of the oxidizer tank was taken before and after a 20 second run with just oxygen. The measured mass was 0.703 kg, corresponding to a flow rate of 35 g/s at an inlet pressure of just over 500 psi. (It should be noted that the scale used to weigh the oxygen bottle measured a 0.703 kg difference after the cold flow. The accuracy of the scale is ±0.01 lbs or ±5 grams.) Calculations run with the same code used to analyze the hotfire results give a total flow of 0.774 kg or an average flow rate of about 37 g/s. Therefore, the calculation and the measurement are within error bars (5-10%) of each other.

Chamber pressure was measured at 1 kHz during the short duration tests using a Viatran (1000 psia) pressure transducer. These pressure transducers have an error of  $\pm 0.15\%$  of full scale (or about 1.5 psi). The system is being upgraded to include a Kistler pressure transducer in order get faster time response data. The two different chamber pressure ranges are achieved by using two separate nozzles. The small nozzle has an area ratio of 3.52, corresponding to a throat diameter of 1.22 cm (0.48 in) and the large nozzle has an area ratio of 2.25, corresponding to a throat diameter of 1.52 cm (0.60 in). Both the contraction from the combustion chamber and exit expansion are accomplished through simple conical expansions. Since thrust level is not a driver in these tests, the same exit diameter of 2.29 cm (0.9 in) is maintained for both nozzles and a decreased area ratio is accepted.

## B. Analytical Chemistry Laboratory

Material properties are tested using the analytical chemistry lab facilities. In this case, three specific instruments were used to conduct the tests presented in Section III. The instruments are commercially available. The test methodology is presented below.

Thermogravimetric Analysis (TGA) was carried out using a TA Q500 TGA instrument configured in the standard mode. A thin piece of wax sample was freshly shaved (razor blade) from the wax material and was placed in the platinum hang-down pan and loaded into the TGA furnace. The sample was heated to 400 °C from room temperature at a ramp rate of 10 °C/min. The sample compartment was purged with GN2 at 100 mL/min throughout the experiment.

The Differential Scanning Calorimetry (DSC) tests were conducted using a TA Q100 DSC instrument configured in Standard DSC mode using a refrigerated cooling system (RCS) accessory. Disk-shaped wax samples were obtained using a round sample punch on a portion of the thin shaved wax material generated in the TGA section above. The wax disks were placed into a tared aluminum DSC pan, and crimp-sealed with an Al DSC sample lid possessing 5 pinholes. The sample pan was quickly cooled from the instrumental default sample chamber temperature (40 °C) to -90 °C and equilibrated for 5 minutes, followed by heating the sample to 150 °C at 10 °C/min. The DSC sample compartment was purged with GN2 (50 mL/min) during the entire DSC experiment.

Thermomechanical analysis (TMA) was carried out using a TA Q400 TMA instrument configured in standard mode with an expansion probe using a probe force of 0.0050 N. A best attempt at generating a regular rectangle section ( $\sim 2$  mm x 2 mm x 7 mm) of each wax sample was carried out using a razor blade and a straight edge. In order to capture the wax material after the sample melt point was surpassed, an Al tray was prepared to place the wax sample into prior to TMA analysis. *Note:* The TMA length was zeroed prior to the wax sample being mounted, but with the prepared Al boat in place on the TMA stage. The sample was equilibrated at -150 °C, and warmed to 100 °C at 5 °C/min. The TMA sample compartment was purged throughout the run using GN2 at 100 mL/min.

## III. Paraffin Material Properties

It has been noted that the chemical composition of paraffin used across industry and academia for hybrid fuel can vary substantially. The paraffin was subjected to several standard tests in order to determine the melting point and coefficient of thermal expansion as well as to investigate the glass transition. A Mars application could require storage and operation over a large range of temperatures, potentially from -100 °C to +50 °C. Suitable performance of the hybrid fuel across this range will minimize the thermal conditioning required, making it a more favorable propulsion option.

Both a dyed (blackened) and neat sample were tested to determine if the dye affects the material properties. Thermogravimetric analysis (TGA), Differential Scanning Calorimetry (DSC), and Thermomechanical Analysis (TMA) tests were performed on the paraffin. Results of these tests showed a slightly lower melting point than previously predicted for the high melt point wax (5560) procured from CandleWic Company. TGA confirmed that there was negligible mass loss due to volatiles (less than 0.35% was lost by the samples as they reached 200 °C). Finally, the coefficient of thermal expansion (CTE,  $\alpha$ ) is presented down to -150 °C.

## C. Volatiles: Thermogravimetric Analysis

Thermogravimetric analysis (TGA) is a method to determine if samples decompose, oxidize or release volatiles with a change in temperature. TGA found the temperature of the extrapolated onset of thermal decomposition (as seen by a significant loss in sample weight) for both samples to be within 1 °C of each other, at 288.19 °C (neat paraffin) and 288.79 °C (blackened paraffin). The results of these tests are presented in Figure 2. This test confirmed that there was no appreciable loss of volatiles in either case. This is shown by a 0.35% reduction in sample mass at they reached 200 °C. This is important to ensure that equipment will not be damaged in further analysis of these materials.

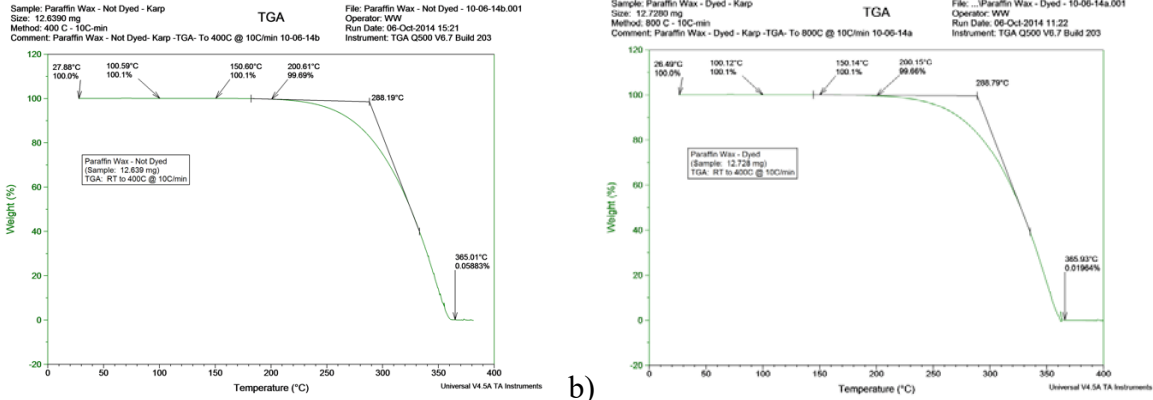


**Figure 2.** TGA of paraffin wax. TGA sample taken to 400 °C at 10 °C/minute.  
 a) Neat paraffin wax. b) Blackened paraffin wax.

#### D. Phase Transition: Differential Scanning Calorimetry (DSC)

DSC measures the amount of heat required to increase the temperature of a sample as a function of temperature and is a way to identify phase transitions. In this case, a phase transition is indicated by a change in the amount of heat required to keep the sample at the same temperature as a reference material. The results of the TGA determined that both wax samples could safely be analyzed by DSC to temperatures up to 200 °C without fear of volatiles depositing in the calorimeter. It is only capable of testing down to -90 °C and not enough information could be gathered around that temperature to determine a glass transition temperature.

DSC runs of the waxes were completed by cooling the samples to -90 °C, holding isothermal for 5 minutes, then heating to 150 °C at a temperature ramp rate of 10 °C/min (Figure 3). The melt point, measured as the extrapolated onset of a sample endotherm, for the neat wax sample was found to be about 5 °C lower than that of the blackened wax sample (44.33 °C vs. 49.50 °C). This comparatively low melt temperature was not expected, since the melt point of the wax is advertised as 160 F (71 °C). The discrepancy is most likely caused by how melt point is defined. The melt point predicted by the vendor can be matched if it is taken as the peak temperature of the endothermic event as opposed to the onset temperature. Defining the melt temperature in this way is common for polymers, but is atypical for metals and organics (like paraffin wax).

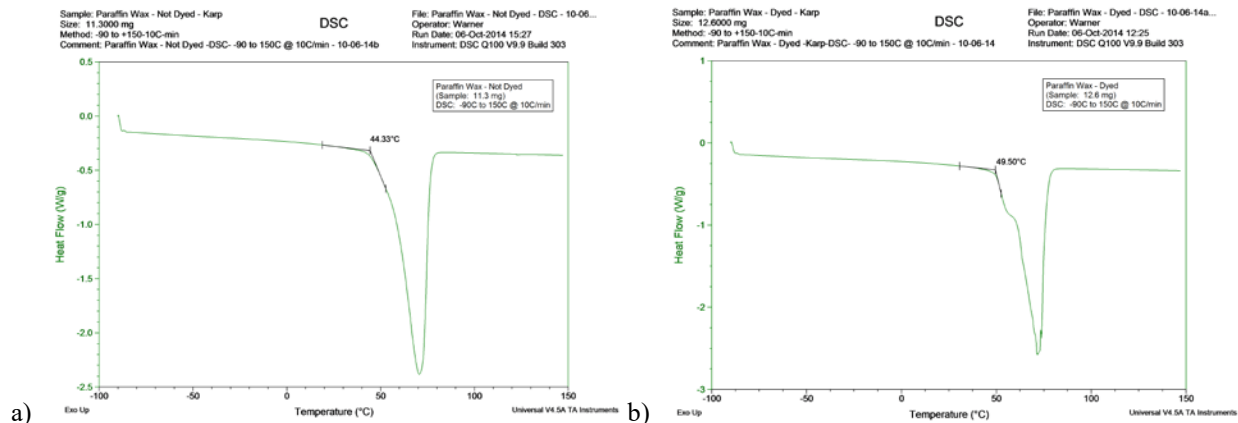


**Figure 3.** DSC of paraffin wax. TGA sample from -90 to +150 °C at 10 °C/minute.  
 a) Neat paraffin wax. b) Blackened paraffin wax.

#### E. Phase Transition and Coefficient of thermal expansion: Thermomechanical Analysis (TMA)

Thermomechanical Analysis (TMA) was used to determine the coefficient of thermal expansion of the wax and in an attempt to determine the glass transition temperature. It was carried out on an approximately rectangular section cut from the wax over the temperature range of -150 °C to 100 °C at a temperature ramp rate of 5 °C/min. The

paraffin samples displayed two somewhat linear CTE regions on either side of around  $-80\text{ }^{\circ}\text{C}$  to  $-90\text{ }^{\circ}\text{C}$ . The onset of a massive sample dimensional loss (peak of the curve) corresponds to the loss of material structural integrity when the melt point of the wax is reached (Figure 4).

These results indicate that paraffin undergoes a very weak glass transition as predicted.<sup>2</sup> The transition is most likely in the neighborhood of  $-90\text{ }^{\circ}\text{C}$  to  $-110\text{ }^{\circ}\text{C}$ , as can be seen by the gentle change in slope in Figure 4. At temperatures below about  $-90\text{ }^{\circ}\text{C}$ , the  $\alpha$  value for both neat and blackened paraffin are very similar,  $63.62\text{ }\mu\text{m}/\text{m}/^{\circ}\text{C}$  and  $62.58\text{ }\mu\text{m}/\text{m}/^{\circ}\text{C}$ , respectively. The coefficients of thermal expansion diverge above temperatures of about  $-70\text{ }^{\circ}\text{C}$ : the neat paraffin has an  $\alpha$  value of  $133.3\text{ }\mu\text{m}/\text{m}/^{\circ}\text{C}$ , while the blackened wax has an  $\alpha$  value of  $177.7\text{ }\mu\text{m}/\text{m}/^{\circ}\text{C}$ . The melting points measured by TMA were in good agreement with those measured by DSC. The TMA melt point for the neat paraffin sample was  $44.58\text{ }^{\circ}\text{C}$  ( $44.33\text{ }^{\circ}\text{C}$  by DSC), and the blackened wax TMA melt point was  $51.53\text{ }^{\circ}\text{C}$  ( $49.50\text{ }^{\circ}\text{C}$  by DSC).

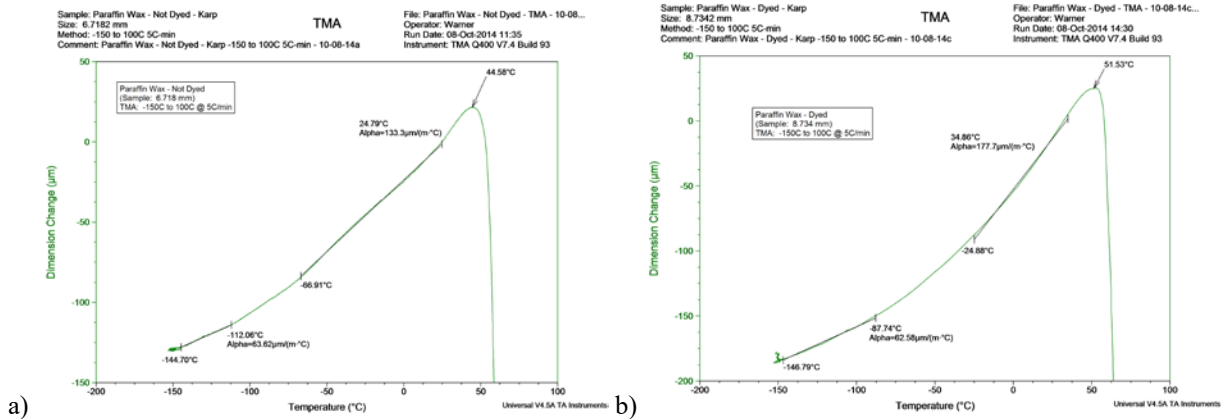


**Figure 4. TMA results of paraffin wax.** TMA sample from  $-150$  to  $+100\text{ }^{\circ}\text{C}$  at  $10\text{ }^{\circ}\text{C}/\text{minute}$ .  
*a) Neat paraffin wax. b) Blackened paraffin wax.*

#### IV. Test Results and Discussion

##### A. Hotfire Test Results

There is substantial flexibility in this test set up and there are many unknowns left for applying hybrid rocket technology to in-space applications. Also, a great deal of data exists for hybrid rockets utilizing blackened paraffin wax and GOx. Therefore, in this series of tests, off nominal conditions are explored, while still enabling comparison to previous work. A low oxidizer mass flux regime is studied to obtain information for future throttling applications across two ranges of chamber pressure: supercritical and subcritical for paraffin wax. The , pressure for paraffin is approximately  $670\text{ kPa}$  ( $97\text{ psi}$ ).<sup>3</sup> Of the eight tests completed to date, four are presented here, two above the critical temperature of paraffin and two below. One additional test is included in the discussion of low oxidizer mass flux as a hint towards behavior in the higher flux regimes. All tests were intended to run for just over three seconds; however, the low-pressure tests quenched combustion after only half the run time. Oxidizer continued to flow for the remainder of the test, as can be seen by the slight increase chamber pressure in tests 6 and 7 until just after 6 seconds (Figures 5b and 5d).

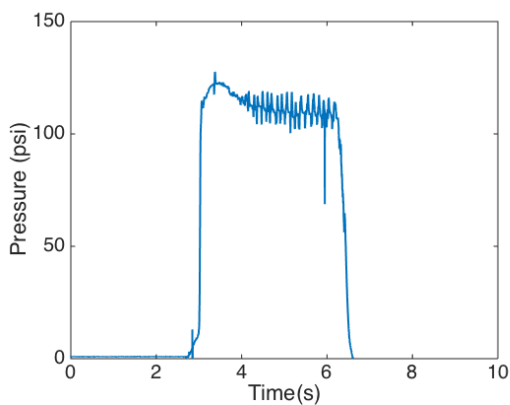
**Table 1: Summary of Test Results**

Test Number	Test Date	Maximum Chamber Pressure ( $P_c$ , psia)	Nozzle	Oxidizer Mass Flow (g/s)	Oxidizer Mass Flux Range ( $G_o$ , g/cm <sup>2</sup> s)	Mass of Fuel Burned (g)	Burn Time (s)	O/F	Average* Regression Rate (mm/s)
5	3/18/2015	122	Small	43	14.3-3.8	131	3.5	1.1	2.9
6	4/29/2015	73	Large	37	13.6-7.0	30	1.3	1.6	2.8
7	5/13/2015	86	Large	45	15.5-7.5	38	1.5	1.8	2.6
8	6/10/2015	142	Small	45	15.5-4.4	114	3.6	1.4	2.3

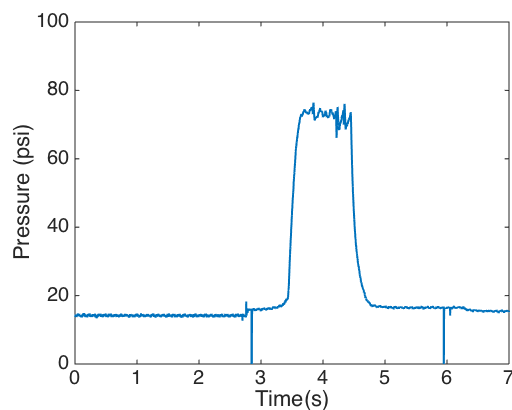
\*Note, the regression rate is both spatially and temporally averaged. It is calculated by taking the difference in the average port diameter (as measured at no fewer than four stations around the fore and aft ends) before and after each test and dividing it by the burn time.

Table 1 summarizes the tests discussed here. The maximum chamber pressure is presented and was selected (by hand) as the maximum pressure not caused by an instability peak. The oxidizer mass flow rate is relatively stable over the 3 second burn time. It is presented as an average to smooth out the noise observed in the pressure data used to calculate this value. The oxidizer mass flux column presents the initial and final values. Measurements of the fuel grain port are made before and after each test to calculate these values. The mass of the fuel grain and insulator is taken before and after each test. No noticeable ablation has been seen in the post combustion chamber since the switch from phenolic was made to graphite after Test 2. The burn time is calculated from the pressure traces. This value and the oxidizer mass flow rate are used to calculate the total oxidizer mass, which in turn is used to determine the average O/F ratio. The regression rate is again an average taken from the difference in fuel grain thickness. One of two nozzles is used for each test. Both were described in the test set up section.

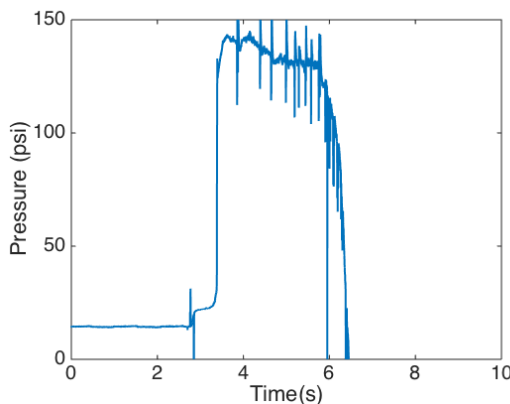
a) Test 5, Supercritical Pressure



b) Test 6, Subcritical Pressure



c) Test 8, Supercritical Pressure



d) Test 7, Subcritical Pressure

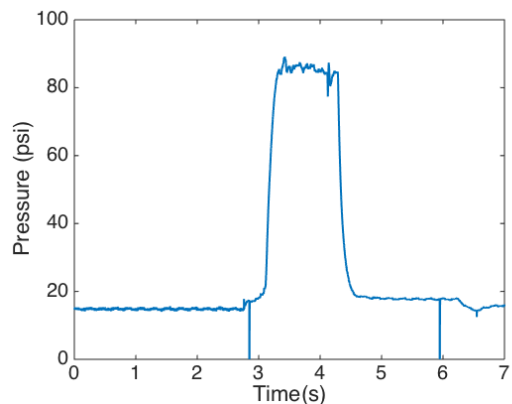


**Figure 5. Chamber Pressures.** Results from four tests. The plots on the left are above the supercritical temperature for paraffin (nozzle with a small throat) and plots on the right are subcritical (nozzle with a large throat).

It should be noted that the length to diameter ratio ( $L/D$ ) of the fuel grain for all of these tests is three, which is much smaller than the range typically predicted to optimize mixing (6-12). The short fuel grains are augmented with a small post combustion chamber. However, the performance is still expected to decrease. Many methods have been employed in other studies to enhance mixing in short configurations such as these (e.g. swirl injection, flow trips). Options such as these were not considered in these preliminary tests, but may be incorporated in the future.

Many previous studies have been completed with gaseous oxygen combustion with paraffin fuels. Figure 3 in Ref. 4 shows a plot of regression rate data over a wide range of oxidizer mass fluxes for SP-1a (a similar, paraffin-based fuel) with gaseous oxygen. Over the range of oxidizer mass fluxes tested at JPL, Ref. 4 gives a range of

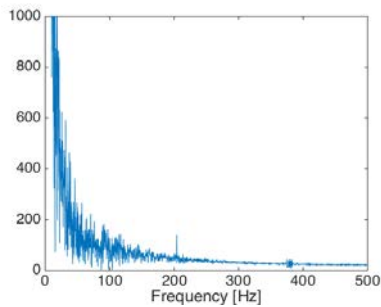
regression rates from about 1-3 mm/s. It can be seen that the regression rates calculated here (given in Table 1) are in family with these measurements, though they trend slightly higher. This is possibly due to the decreased melt temperature measured for this batch of paraffin. It also may just be a byproduct of the way the data was averaged. A pronounced difference in regression rate between the subcritical and supercritical tests was expected, as predicted by Ref. 5. However, the highly averaged regression rates were not substantially different from each other. It is recommended that future tests be conducted in a way that enables multiple regression rates to be measured across smaller ranges of oxidizer mass flux.

## B. Chamber Pressure

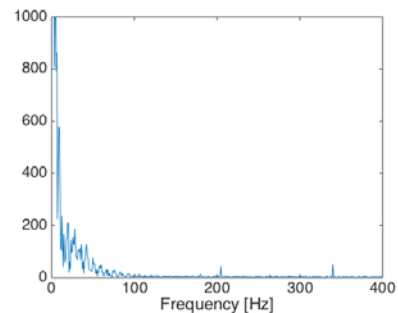
Chamber pressures are presented in Figure 5. They are grouped into two categories: supercritical (chamber pressures above the critical pressure of paraffin, or above about 100 psi) and subcritical (chamber pressures below the critical pressure for paraffin). The top row of tests in Figure 5 had a lower oxidizer inlet pressure and therefore a correspondingly lower oxidizer mass flow rate. However, each category experienced similar behavior.

The supercritical tests have an initial peak in pressure and settle into a region of instability (also see Figure 7). The results from Test 8 were fairly different from the previous tests using similar conditions. So much so that they were nearly excluded. However, these discrepancies can provide information on potential issues. Test 8 was far noisier than the previous tests. This is believed to be at least partially caused by the introduction of new (higher loaded) igniters due to issues with the previous batch. There is potentially a feed system instability because the injector and orifice are so close in area. This will be resolved in the next round of testing.

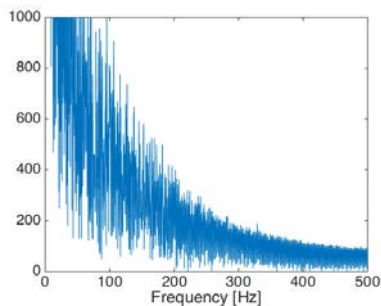
a) Test 5, Supercritical Pressure



b) Test 6, Subcritical Pressure



c) Test 8, Supercritical Pressure



d) Test 7, Subcritical Pressure

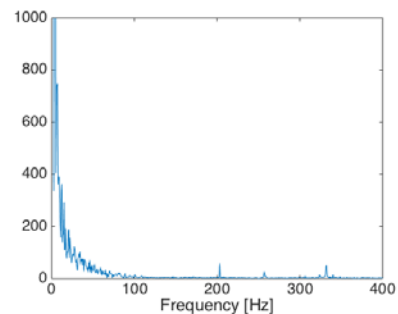


**Figure 6. Fast Fourier Transform.** *Fast Fourier transforms of the four pressure traces. Most of the instability is low frequency as is typical of most hybrid propulsion development programs.*

## C. Instabilities and Transients

There is clearly instability in the chamber pressure traces, especially in tests 5 and 8. Fourier transforms of the pressure traces indicate that these instabilities are predominately low frequency (defined as less than 200 Hz), with small peaks at higher frequency acoustic modes (Figure 6). There are several types of low frequency instabilities: feed system coupled instabilities, chuffing and intrinsic low frequency instabilities (ILFI)<sup>6</sup> and flame-holding instabilities.<sup>7</sup> A transient model of low frequency instabilities, like those observed here, has been presented by Ref. 8. Using Equation 15 from Ref 8, including their value of  $6.39 \times 10^5 \text{ (m/s)}^2$  for  $RT_{avg}$ , (shown as Equation 1 here), the following ranges of frequencies for instabilities in a thermal-combustion-gas coupled system are expected: 9 – 50 Hz for the supercritical pressure cases and 25 – 71 Hz the subcritical cases.

$$f = 0.239 \left( 1 + \frac{1}{O/F} \right) \frac{G_o R T_{avg}}{L P_c} \quad (1)$$

The ignition transient is much longer than expected in the plots shown in Figure 5. It is believed that it takes some time for a combustible mixture of oxygen and paraffin to be reached in the combustion chamber. This is atypical for hybrids operating at nominal conditions. For example, see Figure 7, which has a more reasonable initial oxidizer mass flux.



**Figure 7. Flame shedding during test 6.** *The top image shows normal combustion and the bottom is the flame exiting the combustion chamber during the same test.*

The subcritical pressure tests had a substantial problem maintaining combustion. It appears that the flame detaches at an oxidizer mass flux of about 7-7.5 g/cm<sup>2</sup>s in the subcritical cases. Video of the shut down event shows a visible pulsing of the plume immediately prior to the cessation of combustion. In test 6, three flashes are visible. A comparison of normal combustion to the pulsing is shown in Figure 7. Only a single event is visible in test 7. It is not recommended that such low pressures be used in practical applications.

#### D. Oxidizer Mass Flux

The tests presented here are at particularly low oxidizer mass fluxes. Noticeable instabilities can be seen, especially after the ignition transient is complete. Figure 8 presents a case with roughly 20% higher initial oxidizer mass flow rate (54.6 g/s). This translates to an oxidizer mass flux of 19.1-4.8 g/cm<sup>2</sup>s over the length of the burn. It uses the same injector as the cases in Figure 5; however, this case was run before the addition of the upstream orifice and therefore setting a higher oxidizer mass flow rate. The oxidizer enters the combustion chamber sonically, which can affect mixing. It has the same grain configuration (3:1 L/D) as the previous cases.

The very low frequency (<5 Hz) instability in this pressure trace suggests that this may actually be a chuffing problem.<sup>9</sup> Similar behavior corresponding to large ejecta events was seen at low oxidizer mass fluxes in Ref. 10.

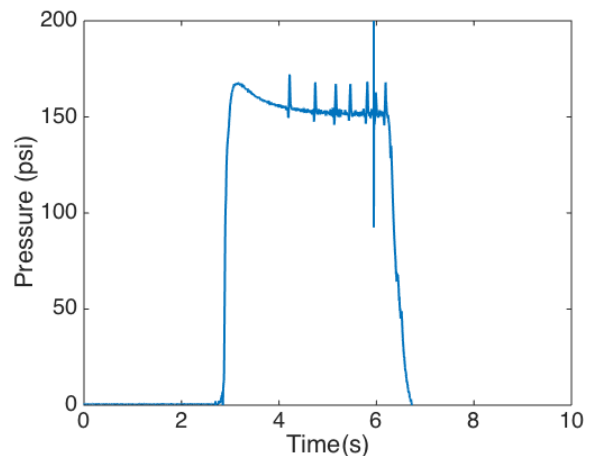


**Figure 8. Chamber pressure from Test 3.** *This test used the same injector as those presented in Figure 5, however, it did without the upstream, sonic orifice. Therefore the oxidizer mass flow is higher than the other cases (~55 g/s).*

## V. Conclusion

Paraffin based hybrid rockets are very promising as in-space motors or as a building block towards human missions to Mars utilizing ISRU oxidizers. Several off-nominal operation regimes were analyzed and issues were

identified for further testing in the short fuel grain and low oxidizer mass flux regime. Instabilities were expected and it is anticipated that modifications to the motor can be made to correct these behaviors as many GOx/paraffin motors have been made to operate stably in the past. This paper provides preliminary test data to begin closing knowledge gaps for configurations and operating regimes not normally used as a means to bound operational parameters. Please note that no mitigation techniques have been employed thus far.

The glass transition temperature of paraffin was investigated and found to be so weak that it could not be strictly determined through the two tests conducted. The differential scanning calorimeter did not detect a transition over its somewhat limited range (down to -90 °C). The thermomechanical analysis potentially detected a weak glass transition in the range of -90 °C to -110 °C. A large coefficient of thermal expansion was measured for paraffin and it was found to vary between blackened and neat paraffin. This will pose a challenge to designing fuel grains for large operational or storage temperature ranges, as expected for ISRU applications.

### Acknowledgments

The research was carried out at the Jet Propulsion Laboratory, California Institute of Technology, under a contract with the National Aeronautics and Space Administration. The authors would like to thank the Jet Propulsion Laboratory for funding this research through its internal Research and Technology Development program. The authors would also like to thank the test team: Lawrence Harma, Matthew Devost, Alex Wolpe, Richard Webster, Alex Luna and William Gavid.

### References

- 
- <sup>1</sup> Chandler, A. A., Gatto, C. E., Nakazono, B., Grayson, K., and Vaughan, D. A., "Hybrid Propulsion In-Situ Resource Utilization Test Facility Development." 50th AIAA/ASME/SAE/ASEE Joint Propulsion Conference. July 28-30, 2014, Cleveland, OH. AIAA 2014-3866.
  - <sup>2</sup> Chandler, A.A., Cantwell, B.J., Hubbard, G. S. and Karabeyoglu, A., "A Two-Stage, Single Port Hybrid Propulsion System for a Mars Ascent Vehicle." 46th AIAA/ASME/SAE/ASEE Joint Propulsion Conference & Exhibit 25 - 28 July 2010, Nashville, TN. AIAA-2010-6635
  - <sup>3</sup> Karabeyoglu, A., Cantwell, B., and Stevens, J., "Evaluation of the Homologous Series of Normal Alkanes as Hybrid Rocket Fuels," 41st AIAA/ASME/SAE/ASEE Joint Propulsion Conference & Exhibit, 10-13 July 2005. Tuscon, Az. AIAA 2005-3908.
  - <sup>4</sup> Karabeyoglu, A., Zilliac, G., Cantwell, B.J., DeZilwa, S., and Castellucci, P., "Scale-Up Tests of High Regression Rate Paraffin-Based Hybrid Rocket Fuels." *J. Prop Power*, Vol. 20, No. 6, pp. 1037-1045, November–December 2004.
  - <sup>5</sup> Muzzy, R.J., "Applied Hybrid Combustion Theory," AIAA/SAE 8<sup>th</sup> Joint Propulsion Specialist Conference, New Orleans, LA, Nov 29- Dec 1, 1972. AIAA Paper Number 72-1143.
  - <sup>6</sup> Chiaverini, M.J. and Kuo, K.K. (ed.), *Fundamentals of Hybrid Rocket Combustion and Propulsion*, Progress in Aeronautics and Astronautic, Vol. 218, AIAA, Virginia, 2007, pp. 351-411.
  - <sup>7</sup> Pucci, J.M., "The Effects of Swirl Injector Design on Hybrid Flame Holding Instability." 38th AIAA/ASME/SAE/ASEE Joint Propulsion Conference & Exhibit, 7-10 July 2002, Indianapolis, Indiana. AIAA 2002-3578
  - <sup>8</sup> Karabeyoglu, M.A., De Zilwa, S., Cantwell, B., Zilliac, Z. "Transient Modeling of Hybrid Rocket Low Frequency Instabilities." 39th AIAA/ASME/SAE/ASEE Joint Propulsion Conference & Exhibit, 20-23 July 2003, Huntsville, AL. AIAA 2003-4463
  - <sup>9</sup> Greiner, B. and Frederick, R.A., "Hybrid Rocket Instability." 29th AIAA/SAE/ASME/ASEE Joint Propulsion Conference, June 28-30, 1993, Monterey, CA. AIAA 93-2553.
  - <sup>10</sup> Jens, E. T., Mechentel, Flora S., Cantwell, B. J., Hubbard, G. S. and Chandler, A. A., "Combustion Visualization of Paraffin-Based Hybrid Rocket Fuel at Elevated Pressures." 50th AIAA/ASME/SAE/ASEE Joint Propulsion Conference, July 28-30, 2014, Cleveland, OH. AIAA 2014-3848